ELSEVIER

PII: S0308-0161(97)00047-1

Int. J. Pres. Ves. & Piping 72 (1997) 203–218

0308-0161/97/$17.00

Stability analysis of a toroidal pipe-reducer under uniform external pressure

Prashanta Dutta,[a] Md. Raisuddin Khan,[b] Md. Abdus Salam Akanda[c] & Md. Wahhaj Uddin[a]

[a]*Mechanical Engineering Department, Bangladesh University of Engineering and Technology, Dhaka Bangladesh*
[b]*Mechanical Engineering Department, Bangladesh Institute of Technology, Chittagong, Bangladesh*
[c]*Institute of Nuclear Science & Technology, Bangladesh Atomic Energy Commission, Dhaka, Bangladesh*

(Received 6 April 1997; accepted 5 May 1997)

The stability of a toroidal pipe-reducer system is determined here from the solution of non-linear governing equations of axisymmetric deformations of shells of revolution. Numerical solutions are obtained by a modified version of the computer program developed by Uddin for solving the governing equations of axisymmetric shells by the multisegment method of integration. The interpretation of instability of the toroidal reducers is based on Thompson's theorems I and II. Critical pressures for the toroidal reduers are calculated over useful ranges of the curvature ratio, the thickness ratio, and the diameter ratio. It has been found that the critical pressure of these reducers varies almost linearly with the diameter ratio and that the long toroidal reducers are prone to local instability near the larger end. But this critical zone occurs near either one of the two ends as the reducer becomes shorter. The results of stability and stress analysis of toroidal pipe-reducers are compared here with those of conical reducers obtained by Ali and parabolic reducers obtained by Rahman. Comparison shows that toroidal reducers develop uniform stresses of lower magnitude compared to the other two. Further, toroidal reducers are found to sustain higher critical pressure than parabolic reducers except at higher diameter ratio. © 1997 Published by Elsevier Science Ltd.

NOMENCLATURE

C, D	Extensional rigidity, bending ridigity
$\bar{C}$	$(1-\nu^2)\xi_e/R$
$\bar{D}$	$1/[12(1-\nu^2)\bar{P}\bar{T}^2\bar{R}]$
E, ν	Young's modulus, Poisson's ratio
H, V	Radial and axial stress resultants
$\bar{H}, \bar{V}$	H/PR, V/PR
h	Shell thickness
k_θ, k_ξ	Changes of curvature of the middle surface of shell
$\bar{k}_\theta, \bar{k}_\xi$	$k_\theta\xi_e$, $k_\xi\xi_e$
$\bar{L}$	$\bar{R}/\bar{P}.\bar{T}$
M_ξ, M_θ	Meridional and circumferential couple resultants
$\bar{M}_\xi, \bar{M}_\theta$	M_ξ/PRh, M_θ/PRh
N_ξ, N_θ	Meridional and circumferential stress resultants
$\bar{N}_\xi, \bar{N}_\theta$	N_ξ/PR, N_θ/PR
$P, \bar{P}$	Outward normal pressure, P/E
$P_c, \bar{P}_c$	Critical pressure, P_c/E
Q	Transverse shear stress resultant
$R, R_1, \bar{R}$	Larger (base) radius, smaller radius of the reducer, ξ_e/R
R_S	Radius of curvature of the toroid
$\bar{R}_1, \bar{R}_s$	Reduction ratio (R_1/R), curvature ratio (R_s/R)
R_ξ, R_θ	Principal radii of curvature of middle surface of shell
$r_0, \bar{r}_0$	Radial distance of a point on undeformed middle surface from the axis of symmetry, r_0/ξ_e
r	r_0+u: radial distance of a point on the deformed middle surface from axis of symmetry
$\bar{T}$	Thickness ratio (R/h)
u, w	Radial displacement, axial displacement
$\bar{u}, \bar{w}$	uEh/PR^2, wEh/PR^2
z_0, z	Axial distance of a point on undeformed middle surface of shell, z_0+w
α, α_0	Parameter of meridian of deformed shell, α_0 corresponds to undeformed state
$\beta, \bar{\beta}$	Angle of rotation of normal after deformation, β

ξ_ξ, ε_θ	Middle surface strains
$\bar{\varepsilon}_\xi$, $\bar{\varepsilon}_\theta$	$\varepsilon_\xi Eh\xi_e/PR^2$, $\varepsilon_\theta Eh\xi_e/PR^2$
ξ, $\bar{\xi}$	Distance measured along meridian, ξ/ξ_e
ξ_e	Total meridional length, between the centre of the smaller end and the larger end junction
ϕ_0, ϕ	Angle between normal and axis of symmetry before deformation (meridional angle), $\phi_0 - \beta$
σ_{ai}, σ_{ao}	Meridional stresses at the inner and outer wall surfaces of the reducer
σ_{ci}, σ_{co}	Circumferential stress at the inner and outer wall surfaces of the reducer
$(\ldots)'$	Derivative with respect to ξ or $\bar{\xi}$
$\bar{\sigma}_{ai}$, $\bar{\sigma}_{ao}$	$\sigma_{ai}/(PR/h)$, $\sigma_{ao}/(PR/h)$
$\bar{\sigma}_{ci}$, $\bar{\sigma}_{co}$	$\sigma_{ci}/(PR/h)$, $\sigma_{co}/(PR/h)$

INTRODUCTION

Large-size pipe-reducers can be considered as thin axisymmetric shells. These thin shells, in general, can transmit the surface load primarily through the uniformly distributed in-plane membrane forces by virtue of their curved surfaces, without the action of bending or twisting. This property makes them, as a rule, a much more rigid and more economical structure than a plate. Further, shells are becoming thinner with the passage of time because of the improving strength of materials and the development of new stronger materials. Consequently, to-day's thinner structures are more prone to failue due to instability than due to strength. Buckling usually results in abrupt changes in the shape of the structures which ultimately leads them to failure because of the enormous deformations of an initially stable equilibrium position.

Analysis of thin shells having sharp changes in meridional curvature invariably passes into the domain of non-linear mathematics. That linear shell analysis fails to give proper informations about the shell stresses and deformations in many problems can be seen in recent papers on the non-linear shell analysis of Thurston.[1,2] For this reason, the use of non-linear theory has become rather widely accepted as a plausible basis for predictions of elastic strengths and stability of shells of various geometries. It should be mentioned here that the stability analysis is justified for thinner reducers of larger reduction ratio. The present analysis is thus for thinner reducers with varying diameter ratio.

Non-linear shell analysis involves complex mathematics and can not be solved in closed form. For that reason most of the theoretical works on shell analysis are based on various approximations. These include approximations in the derivation of the governing equations, in the presentation of the geometry of the undeformed shape, in devising methods of solutions of the governing equations and, finally, in obtaining the solutions of the governing algebraic and differential equations by using some numerical techniques.

Finite element and finite difference techniques are most often used for solving non-linear problems of solid mechanics.[3–11] Some of the general purpose computer codes developed on these methods are BOSOR4,[12] BOSOR5,[13] ANSR, and STAGSC[14] for shells of revolution. A critical review of such programs, namely of BOSOR4 and BOSOR5, is presented in Refs [15, 16]. To eliminate the drawbacks of the above computer codes, Uddin[17] has developed a computer program for the analysis of composite shells of revolution. He has obtained extensive numerical results on spherical, ellipsoidal, conical and composite head pressure vessels based on both the linear and non-linear theories and also on the buckling pressures of general spherical shells and semi-ellipsoidal shells.[15–20] In all these investigations, he has shown the conservativeness of linear theory and demonstrated the superiority of non-linear analysis. Later Haque[16,21] carried out the buckling analysis of ellipsoidal shells of revolution under external pressure and Rahman[22] extended it to include imperfection in geometry.

Ali[23] carried out the stability and stress analysis of general truncated conical shells, used as pipe-reducers. In his work, Ali[23] pointed out that the critical load for a conical reducer decreases almost linearly with increasing apex angle of the conical frustum. Rahman[24] analysed the stability and stresses of parabolic pipe-reducers. In his investigation, Rahman showed that doubly curved truncated parabolic shells can sustain a higher critical load than singly curved conical frustum. But fabrication of a parabolic shell is quite difficult. Instead of a toroidal shell, another doubly curved shell may be analysed for its suitability under external loading.

The present study deals with the stability analysis of toroidal shells. In the present analysis, the governing non-linear equations of axisymmetric deformations of shell of revolution which ensure the unique state of the lowest potential energy are solved for increasing value of load parameter. At each load step the appearance of the second mode is looked for. The onset of the first bifurcation point is usually indicated by a substantial increase in the displacements and stresses of the shell for a very small increase of the load parameter. In the case of snap buckling at the bifurcation point any increase in load, however small, produces enormous deformation and thus the numerical technique used here fails to converge to any solution.

The multisegment method of integration of Kalnins[25] is used here to solve the non-linear governing equations of the axisymmetric shells. The main advantage of this method over the others is that the solution is obtained with uniform accuracy with respect to mesh size. Further any discontinuity, either

in geometry or in loading, can be easily handled by requiring that the end points of the segments coincide with the location of discontinuities.

GOVERNING EQUATIONS FOR ANALYSIS OF TOROIDAL REDUCERS

Non-linear governing equations for the axisymmetric buckling of toroidal reducers, based on Reissner's large deflection theory of shells,[26,27] are derived and presented here after necessary modifications. The variables and shell parameters are defined in Figs 1 and 2. The critical pressure for a particular reducer is interpreted here from the observation of the bifurcation point on its fundamental equilibrium configuration path. In case of snap buckling, the bifurcation point was further confirmed by the failure of the technique to converge even for a very small increase of the load parameter.

In determining the critical pressure, the equilibrium configuration path is traced against increasing load. Here the external pressure is increased by small increments and the appearance of a second mode is looked for. The appearance of the second mode always corresponds to the critical loading. Here the critical pressures are evaluated for different toroidal reducers with varying values of the diameter ratio, the thickness ratio and the curvature ratio. The governing equations in terms of variables in Figs 1 and 2 are

$$\bar{\varepsilon}_\theta = \bar{u}/\bar{r}_0 \tag{1a}$$

$$\phi = \phi_0 - \bar{\beta} \tag{1b}$$

$$\bar{k}_\theta = (\sin\phi_0 - \sin\phi)/\bar{r}_0 \tag{1c}$$

$$\bar{N}_\xi = \bar{H}\cos\phi + \bar{V}\sin\phi \tag{1d}$$

$$\bar{\varepsilon}_\xi = \bar{C}\bar{N}_\xi - \nu\bar{\varepsilon}_\theta \tag{1e}$$

$$\bar{k}_\xi = \bar{M}_\xi/\bar{D} - \nu\bar{k}_\theta \tag{1f}$$

$$\bar{N}_\theta = (\bar{\varepsilon}_\theta + \nu\bar{\varepsilon}_\xi)/\bar{C} \tag{1g}$$

$$\bar{M}_\theta = \bar{D}(\bar{k}_\theta + \nu\bar{\varepsilon}_\xi) \tag{1h}$$

$$\bar{\alpha} = \bar{L} + \bar{\varepsilon}_\xi \tag{1i}$$

$$\bar{r} = \bar{L}\,.\,\bar{r}_0 + \bar{u} \tag{1j}$$

$$\bar{w}' = \bar{\alpha}\sin\phi - \bar{L}\sin\phi_0 \tag{1k}$$

$$\bar{u}' = \bar{\alpha}\cos\phi - \bar{L}\cos\phi_0 \tag{1l}$$

$$\bar{\beta}' = \bar{k}_\xi \tag{1m}$$

$$\bar{V}' = -\bar{\alpha}\cos\phi(\bar{V}/\bar{r} - \bar{P}\bar{T}) \tag{1n}$$

$$\bar{H}' = -\bar{\alpha}(\bar{H}\cos\phi - \bar{N}_0)/\bar{r} + \bar{P},\ \bar{T}\sin\phi) \tag{1o}$$

$$\bar{M}'_\xi = \bar{\alpha}\cos\phi(\bar{M}_\theta - \bar{M}_\xi)/\bar{r} - \bar{\alpha}\bar{P}\bar{T}^2(\bar{H}\sin\phi - \bar{V}\cos\phi) \tag{1p}$$

Equations (1) are arranged in such a way that, when evaluated serially they are in terms of the six fundamental variables $\bar{u}$, $\bar{w}$, $\bar{\beta}$, $\bar{v}$, $\bar{h}$, and $\bar{M}_\xi$.

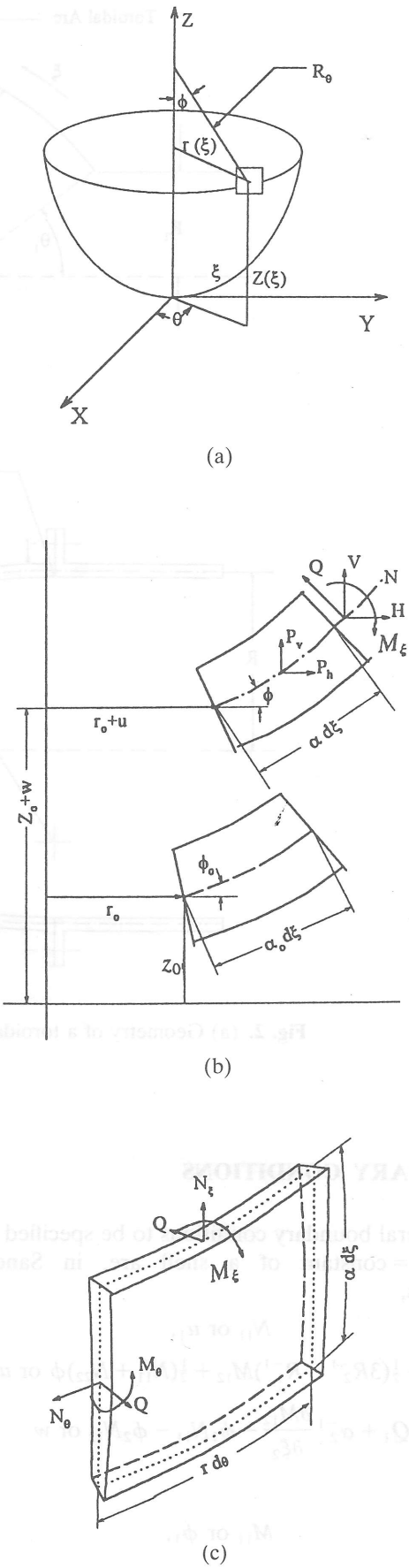

Fig. 1. (a) Middle surface of a shell. (b) Side view of element of shell in deformed and undeformed states. (c) Element of shell showing stress resultants and couples.

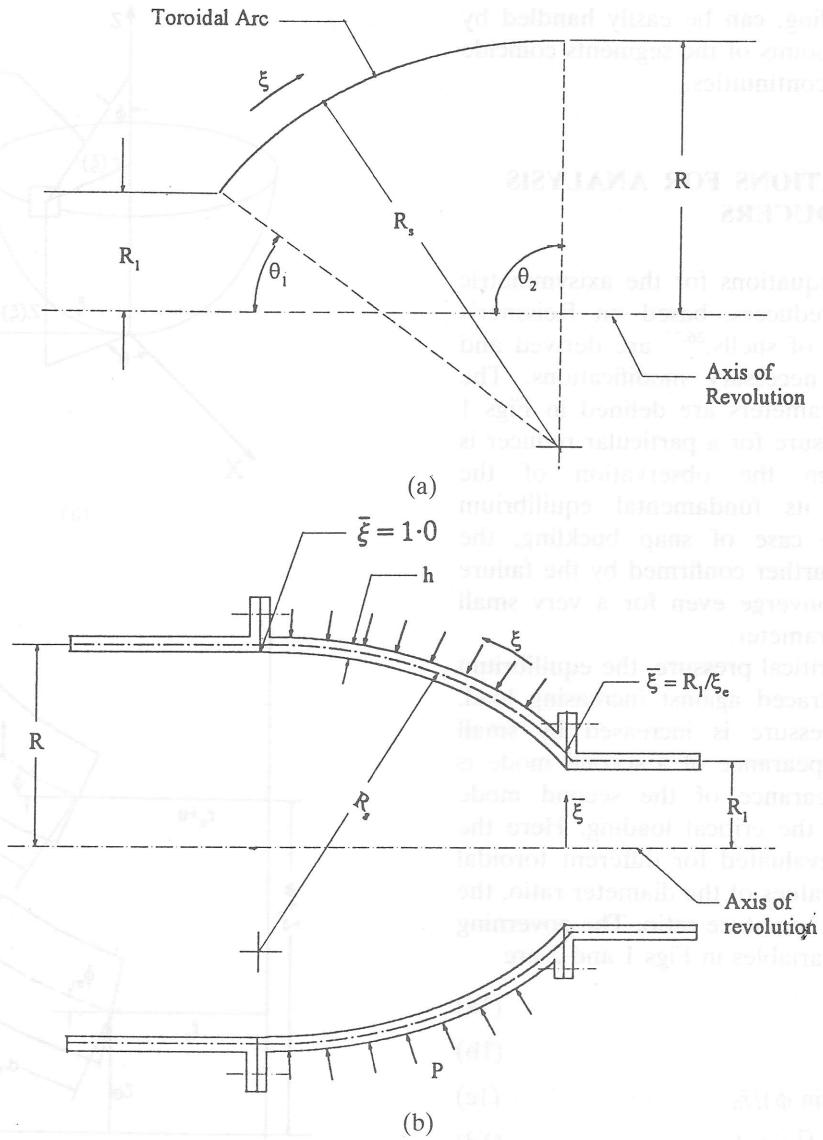

Fig. 2. (a) Geometry of a toroidal reducer. (b) Toroidal reducer with clamped edge.

BOUNDARY CONDITIONS

The general boundary conditions to be specified on an edge $\xi_1 = \text{constant}$ of a shell are, in Sander's[28] notations,

$$N_{11} \text{ or } u_1,$$

$$N_{12} + \tfrac{1}{2}(3R_2^{-1} - R_1^{-1})M_{12} + \tfrac{1}{2}(N_{11} + N_{22})\phi \text{ or } u_2,$$

$$Q_1 + \alpha_2^{-1}\frac{\partial M_{12}}{\partial \xi_2} - \phi_1 N_{11} - \phi_2 N_{12} \text{ or } w \qquad (2a)$$

and

$$M_{11} \text{ or } \phi_1,$$

where N and M are the stress and couple resultants; ϕs are the rotations about respective axes; u and w are tangential and normal displacement components; ξ_1 and ξ_2 are the shell coordinates along the principal lines of curvature.

For axisymmetric deformations of shells of revolution they reduce to

$$N_{11} \text{ or } u_1,$$

$$Q_1 - \phi_1 N_{11} \text{ or } w, \qquad (2b)$$

and

$$M_{11} \text{ or } \phi_1,$$

on an edge $\xi_1 = \text{constant}$. From (2b) it is seen that the boundary conditions consist of the specification of rotational, tangential and normal restraints at the edge. But in most of the practical shell problems the conditions of the horizontal and vertical restraints are known rather than those of the normal and tangential

restraints. So it is preferable to specify the boundary conditions in terms of the horizontal and vertical restraints from the point of view of practical application. Under this condition, the boundary conditions will be in terms of

$$H \text{ or } u,$$
$$M_\xi \text{ or } \beta, \tag{2c}$$

and

$$V \text{ or } w,$$

on the edge $\xi = \text{constant}$. Therefore, for both-ends flanged toroidal reducers the boundary conditions are

$$u = 0, \quad w = 0, \quad \beta = 0 \quad \text{at both the ends.}$$

METHOD OF ANALYSIS

The steps followed in finding the critical pressure are as follows:

i. The linear governing equations of the shell are solved by the multisegment method of integration as developed by Kalnins and Lestingi.[25] With the linear solution providing initial values to the dependent variables, the non-linear equations are solved by the process of iteration at the initially assigned load.
ii. The non-linear equations are then repeatedly solved for increasing values of the load parameter while the initial values for iteration process at any step of load parameter are provided by the solution for immediate previous step of loading.
iii. If any step of the scheme in increasing the load parameter in steps the iteration process fails to converge, then it first subtracts the previous load increment from the current loading, halves the load increment and adds it to the previous loading to arrive at the new normalized loading. In this way the equilibrium configuration path is traced against increased loading.
iv. The critical pressure is anticipated from the load-displacement curves. The equilibrium configuration path is traced against increasing loading and the appearance of a secondary mode of deformation is searched. This appearance of a second mode always corresponds to the bifurcation point as pointed out by Thompson.[29]

RESULTS AND DISCUSSION

The present investigation uses the following parameters to describe the toroidal reducers: (a) thickness ratio $\bar{T}$—the ratio of larger-end radius to the thickness of the reducer, (b) reduction ratio $\bar{R}_1$—the ratio of smaller-end to larger-end radii, (c) curvature ratio $\bar{R}_s$—the ratio of the radius of toroidal arc to the radius of larger-end. To obtain the solutions of different reducers, any two of the parameters are kept constant while the third is varied. In the present study, the thickness ratio and the reduction ratio are kept constant and the curvature ratio is varied within an appropriate range. Then either the value of $\bar{T}$ or $\bar{R}_1$ is varied and the solution is obtained again for the useful range of $\bar{R}_s$. In this study the curvature ratio $\bar{R}_s$ ranges from 1·5 to 2·5. The values of $\bar{T}$ and $\bar{R}_1$ studied here are: $\bar{T} = 500$, 1000, 1500 and $\bar{R}_1 = 0{\cdot}3$, 0·5, 0·7 and 0·9. The critical pressure of the reducers for a given value of thickness ratio is plotted against reduction ratio for different values of the curvature ratio ($\bar{R}_s = 1{\cdot}5$, 2·0, 2·5) in Fig. 3(a–c). Figure 3 shows that critical pressure increases with increasing reduction ratio at a constant curvature ratio as well as with increasing curvature ratio at constant reduction ratio. That is, the larger is the reduction ratio of the reducer the higher is its ability of sustaining external pressure. The critical pressure of the reducers for a given curvature ratio is plotted against reduction ratio in Fig. 3(d) for thickness ratios 500, 1000 and 1500. From this figure it is evident that critical pressure varies linearly with reduction ratio and thickness ratio, linear empirical formula for critical pressure as a function of reduction ratio can be used for the toroidal reducers. It should be noted that if the reduction ratio and thickness ratio are kept constant, the meridional length increases with the increase of curvature ratio. Consequently, for a given reduction ratio and thickness ratio, the critical pressure increases with increase of curvature ratio as shown in Fig. 3. At higher curvature ratio, it behaves like a cylindrical shell.

Table 1 shows a comparison of critical pressures of the conical, parabolic and toroidal pipe-reducers having identical edge conditions. It presents the critical pressures for conical pipe-reducers of an apex angle of 60° and for toroidal pipe-reducers of a curvature ratio, $\bar{R}_s = 2{\cdot}5$. As seen from this table, for a reduction ratio of 0·5 and a thickness ratio of 500, the critical pressure of toroidal reducers is 1·7 times greater than that of conical reducers of an apex angle of 60° and 1·03 times greater than that of parabolic reducers.

The superiority of the toroidal reducer over conical reducer regarding stability becomes more significant with increasing thickness ratio and increasing reduction ratio. For example, for $\bar{T} = 1500$ and $\bar{R}_1 = 0{\cdot}7$, the critical load for a toroidal reducer is 2·1 times that of a conical reducer of an apex angle of 60°. It should be mentioned here that the stability of a conical reducer decreases as the apex angle increases.[1] On the other hand, Table 1 shows that toroidal reducers are slightly more stable than parabolic reducers for a

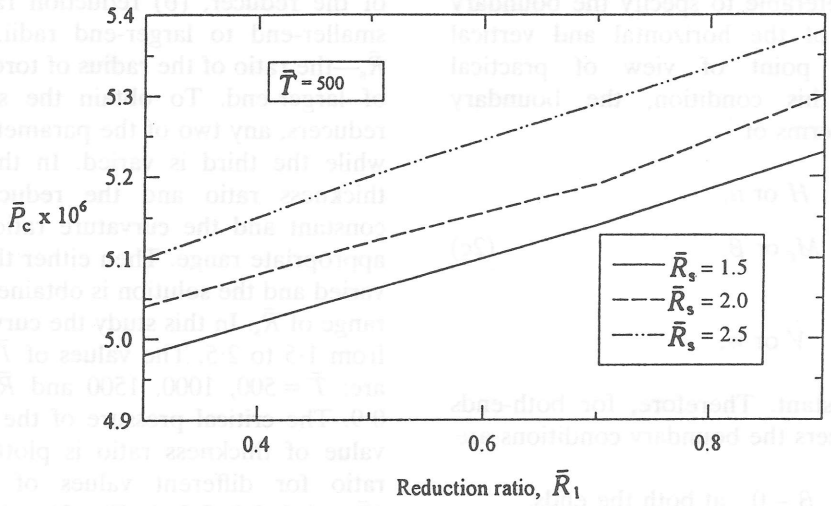

(a)

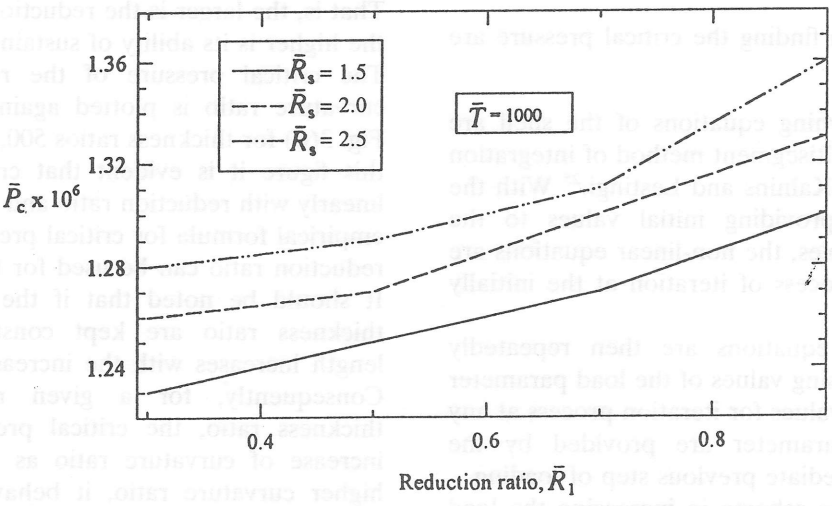

(b)

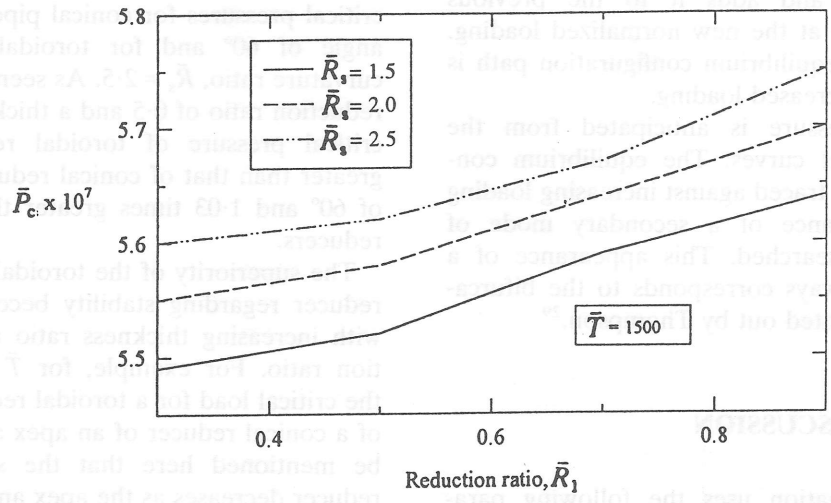

(c)

Fig. 3. Critical load of toroidal reducer for (a)–(c) varying reduction ratio, (d) different thickness ratios.

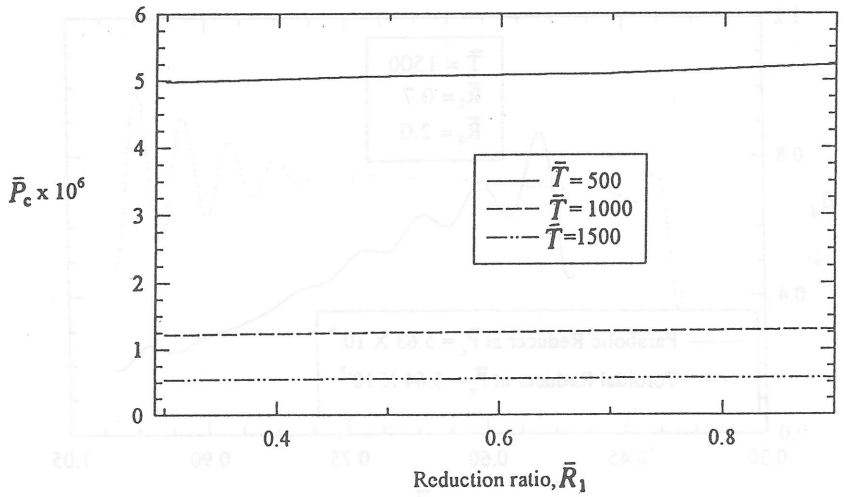

(d)

Fig. 3. (*Continued.*)

Table 1. Comparison of critical pressure of toroidal, parabolic and conical pipe-reducers with clamped edges for different thickness ratios

Thickness ratio T	Reduction ratio $\bar{R}_1$	Critical pressure, $\bar{P}_c \times 10^{-7}$		
		Conical reducer of apex angle 60°	Parabolic reducer	Toroidal reducer of $\bar{R}_s = 2{\cdot}5$
500	0·3	—	50·00	51·00
	0·5	31·00	51·00	52·60
	0·7	27·00	55·00	52·90
	0·9	—	100·00	55·50
1000	0·3	—	11·30	12·80
	0·5	7·00	11·40	12·90
	0·7	6·40	12·40	13·10
	0·9	—	19·30	13·70
1500	0·3	—	5·02	5·60
	0·5	2·90	5·30	5·62
	0·7	2·70	5·62	5·67
	0·9	—	9·60	5·81

given pressure except at higher reduction ratio ($\bar{R}_1 = 0{\cdot}9$). For thickness ratio $\bar{T} = 1000$ and reduction ratio $\bar{R}_1 = 0{\cdot}7$, the critical pressure of the toroidal reducers are 1·05 times of that of parabolic reducers. But, at the same time, for thickness ratio $\bar{T} = 1000$ and reduction ratio $\bar{R}_1 = 0{\cdot}9$, the critical pressure of parabolic reducers is 1·4 times that of toroidal reducers of identical parameters. Therefore, at higher reduction ratio, toroidal reducers are preferable to parabolic reducers.

The stresses under uniform external pressure in a toroidal reducer and in an identical parabolic reducer, having the same thickness ratio and reduction ratio, are presented in Figs 4 and 5. It should be mentioned here that the same clamp-edged boundary conditions are considered for the comparison. From the above mentioned figures, it is evident that parabolic reducers develop stresses of much lower magnitude compared to toroidal reducers, especially at the larger-end. The magnitude and distribution of stress are almost identical at the smaller end for both types of reducer, if they are long. For short parabolic reducers the stress at the smaller end is large than that at the larger end as in Fig. 4(a–d). On the other hand, for long toroidal reducers, the stresses are high at both the ends, but highest at the larger end, as shown in Fig. 5(a–d).

For toroidal reducers, the non-dimensional circumferential stresses ($\bar{\sigma}_{ci}$ and $\bar{c}_{co}$) remain almost constant or fluctuate within a very small range along the entire meridional length. But the circumferential stresses fluctuate widely at the two ends. From Figs 4(a, b) and 5(a, b) it is found that circumferential stress has a greater magnitude near the larger ends. But the circumferential stress distribution in a parabolic reducer decreases along the reducer's meridian from smaller end to larger end.

The pattern of non-dimensional meridional stress distribution is almost identical in both the parabolic and torioidal reducers having identical parameters and boundary conditions as seen in Figs 4(c, d) and 5(c, d). For a toroidal reducer, the non-dimensional meridional stress at the larger end is slightly greater in magnitude than that at the smaller end. On the other hand, the non-dimensional meridional stress level at the smaller end is higher than that at the larger end in a parabolic reducer, shown in Figs 4(c) and 5(c). It has been found that under uniform external pressure the meridional stress at the inner surface is of the highest magnitude among the four components of stresses (σ_{ci}, σ_{co}, σ_{ai}, σ_{ao}) in both the reducers. It is also seen from Fig. 4(c) that the maximum non-dimensional meridional stress occurs at the inner surface, and the value of this stress is 1·6 at the smaller end and 0·4 at the larger end in a parabolic reducer. But for an identical toroidal reducer the same stress is 1·4 at the

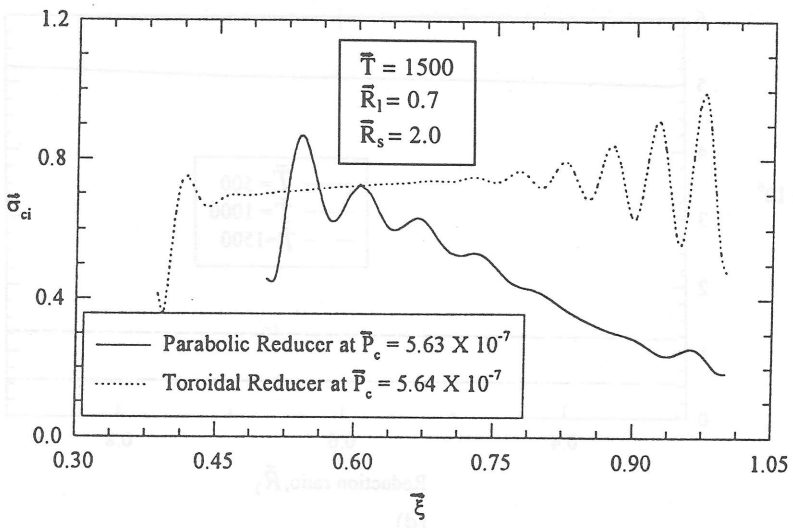

(a)

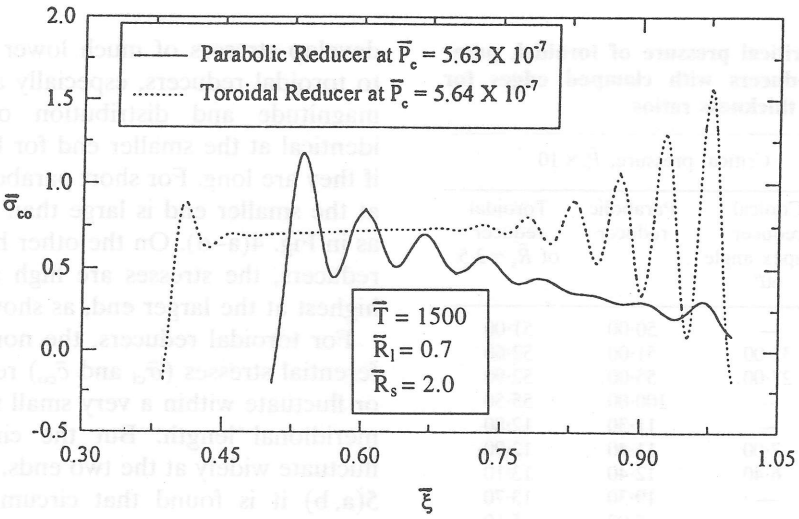

(b)

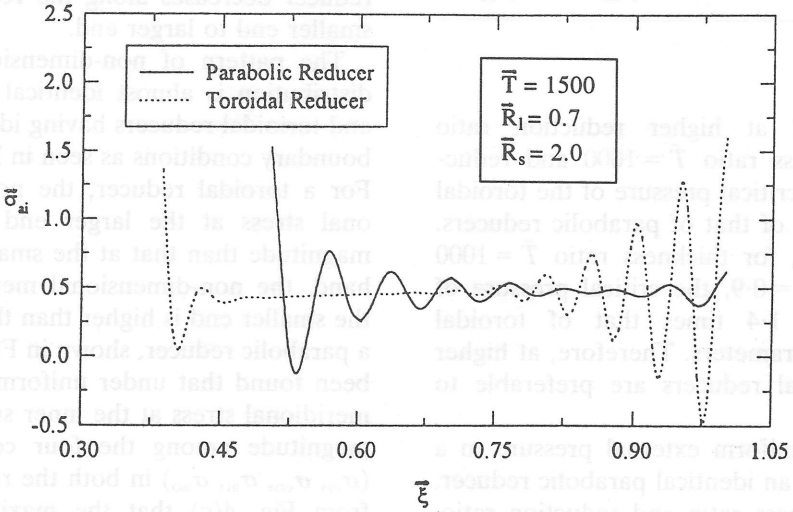

(c)

Fig. 4. Non-dimensional circumferential stresses at (a) the inner surface of parabolic and toroidal reducers, (b) the outer surface of parabolic and toroidal reducers, (c) non-dimensional meridional stresses at the inner surfaces of parabolic and toroidal reducers at $P_c = 5.63 \times 10^{-7}$, (d) non-dimensional meridional stresses at the outer surfaces of parabolic and toroidal reducers.

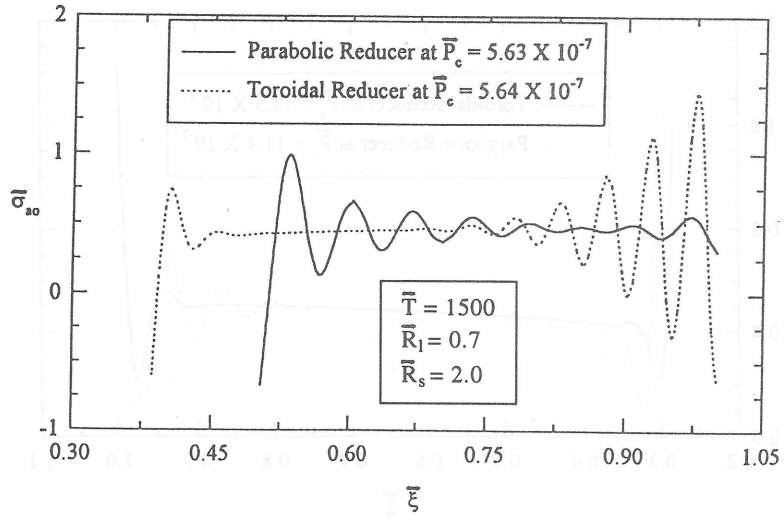

(d)

Fig. 4. (*Continued.*)

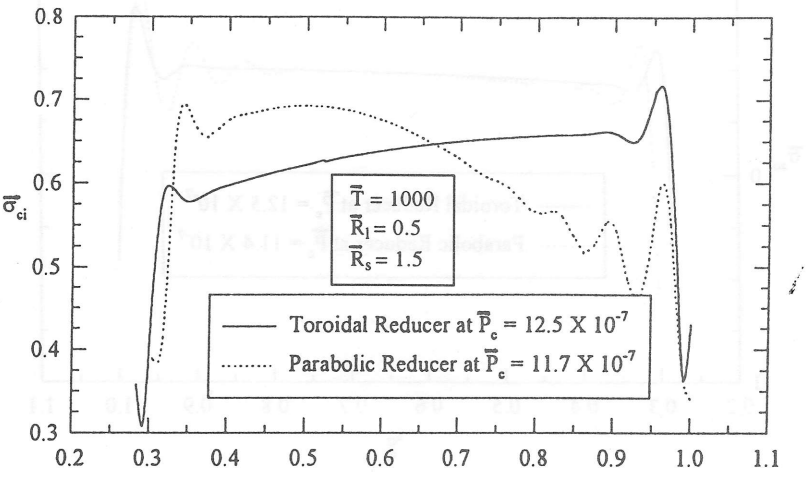

(a)

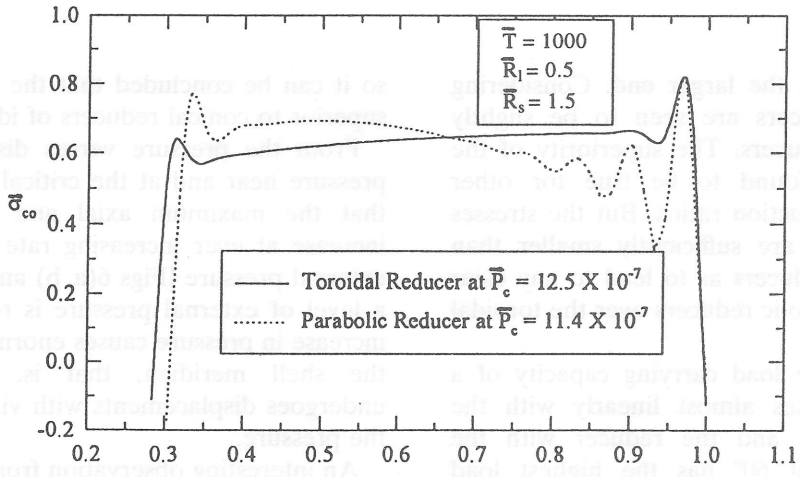

(b)

Fig. 5. (a) Non-dimensional circumferential stresses at the inner surface of parabolic and toroidal reducers, (b) non-dimensional circumferential stresses at the outer surface surface of parabolic and toroidal reducers, (c) meridional stresses at inner surfaces of parabolic and toroidal reducers, (d) meridional stresses at outer surfaces of parabolic and toroidal reducers.

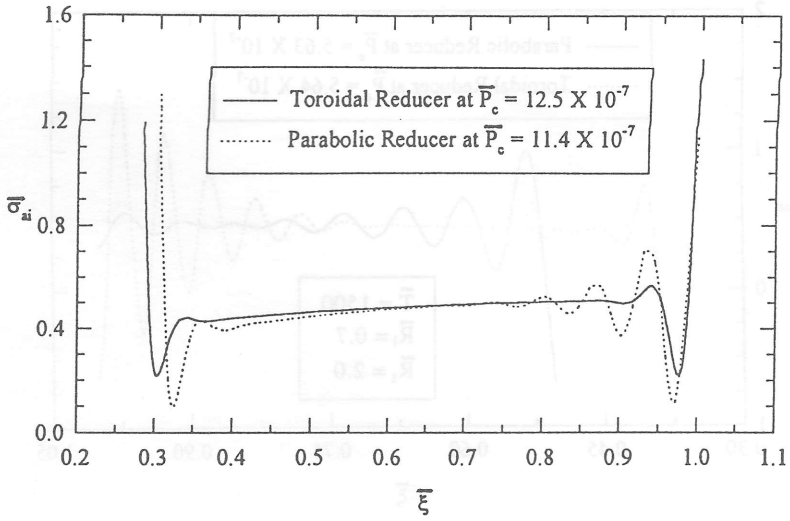

(c)

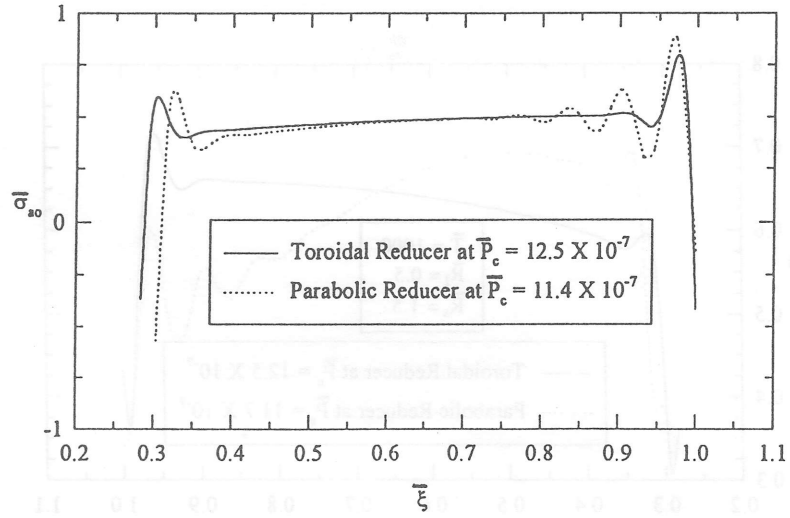

(d)

Fig. 5. (*Continued.*)

smaller end and 1·65 at the larger end. Considering stresses, parabolic reducers are seen to be slightly superior to toroidal reducers. The superiority of the parabolic reducers is found to be true for other thickness ratios and reduction ratios. But the stresses in a parabolic reducer are sufficiently smaller than those in the toroidal reducers as to lead to any clear preference for the parabolic reducers over the toroidal ones.

Ali[23] showed that the load carrying capacity of a conical reducer decreases almost linearly with the increase of apex angle and the reducer with the optimum apex angle at 60° has the highest load carrying capacity. But Rahman[24,30] showed that the stresses in a conical nozzle of 60° apex angle are 2·0–2·5 times higher than those of parabolic reducer. As the maximum stress developed in the toroidal reducers is almost close to that of parabolic reducer, so it can be concluded that the toroidal reducers are superior to conical reducers of identical parameters.

From the pressure versus displacement plots, for pressure near and at the critical state, it can be seen that the maximum axial and radial displacements increase at ever increasing rate with the increase of external pressure [Figs 6(a, b) and 7(a, b)]. Eventually a level of external pressure is reached when a small increase in pressure causes enormous displacements of the shell meridian, that is, the shell meridian undergoes displacements with virtually no increase in the pressure.

An interesting observation from the present analysis is that long toroidal reducers are prone to local instability at the larger end as shown in the buckled configurations of the reducers in Fig. 7(c). Here the adjacent material points on the shell meridian are severely displaced in opposite directions resulting in

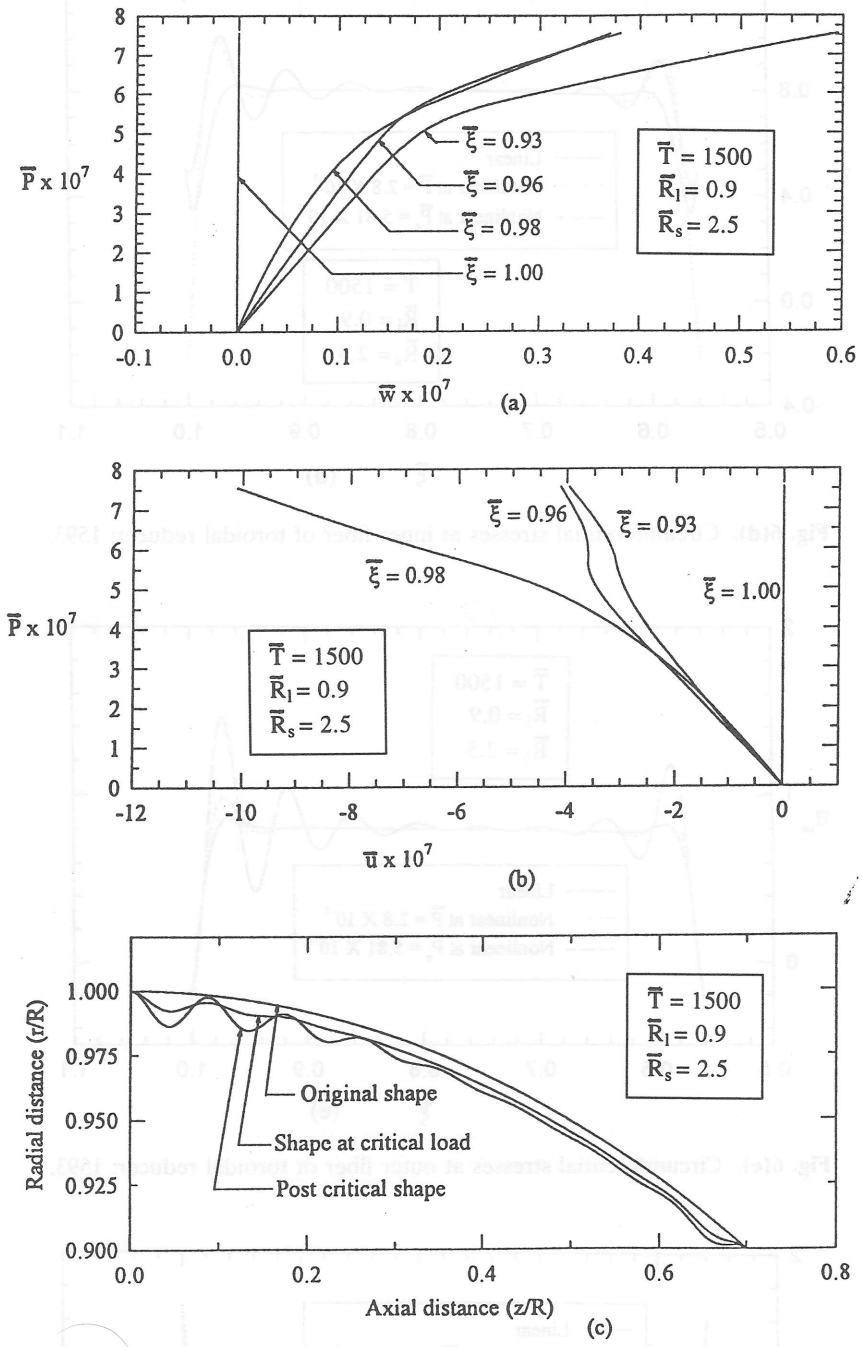

Fig. 6. (a) Axial displacements, (b) radial displacements and (c) buckled configuration of toroidal reducer.

crooked deformation of the reducers near the larger end. On the other hand, short toroidal reducers are most critically stressed both near the larger end as well as near the smaller end as seen in Fig. 6(c). Thus short toroidal reducers are prone to local instability at the two ends. It should be mentioned here that for both long and short reducers the intermediate part of shell meridian remains unaffected.

The stress variations along the shell meridian in the reducer of $\bar{T} = 1500$, $\bar{R}_1 = 0{\cdot}9$ and $\bar{R}_s = 2{\cdot}5$ and also in the reducer of $\bar{T} = 1500$, $\bar{R}_1 = 0{\cdot}3$ and $\bar{R}_s = 2{\cdot}0$, shown on Figs 6(d–g) and 7(d–g), are in complete harmony with their failure pattern as indicated in Figs 6(c) and 7(c). It is observed that, in a long reducer, the materials near the larger end are most critically stressed as shown in Fig. 7(d–g). Conversely, in a short reducer, the critical zone spreads towards both the ends as seen in Fig. 6(d–g), indicating the likelihood of local instability near the two ends. Therefore, longer toroidal reducers have buckling tendency near the larger end. On the other hand, short reducers are weak at both the ends. Further,

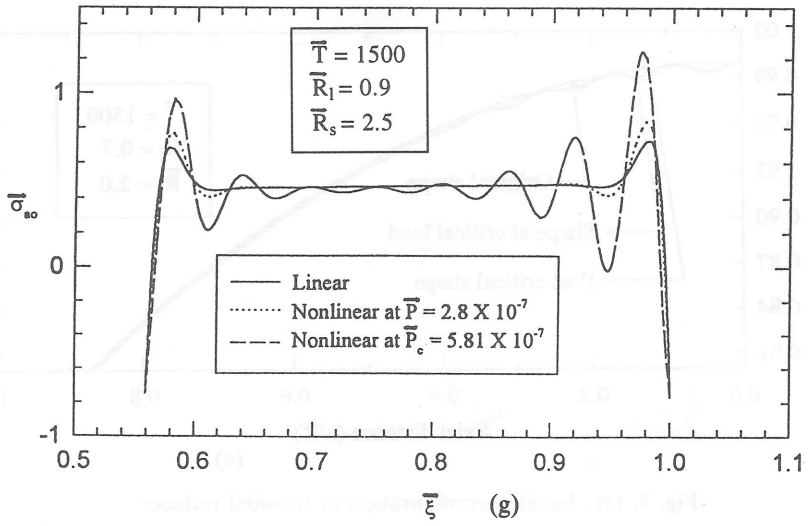

Fig. 6(g). Meridional stresses at outer fiber of toroidal reducer.

increasing reduction ratio increases the load bearing capacity.

From this study it is observed that elastic buckling is more likely to occur in thin shells prior to yielding than in thick shells. As for example, at the critical pressure $\bar{P}_c = 5{\cdot}81 \times 10^{-7}$ of the toroidal reducer of $\bar{R}_s = 2{\cdot}5$, $\bar{R}_1 = 0{\cdot}9$, and $\bar{T} = 1500$, the maximum non-dimensional stress, $\sigma/(PR/h)$, is the meridional stress of the inner fiber at the larger end, $\bar{\xi} = 1{\cdot}0$, Fig. 6(f). Its value is 1·62. For steel, the actual value of the stress comes out to be 292·2 MPa. The yield strength of the medium quality steel is as high as 1200 MPa.

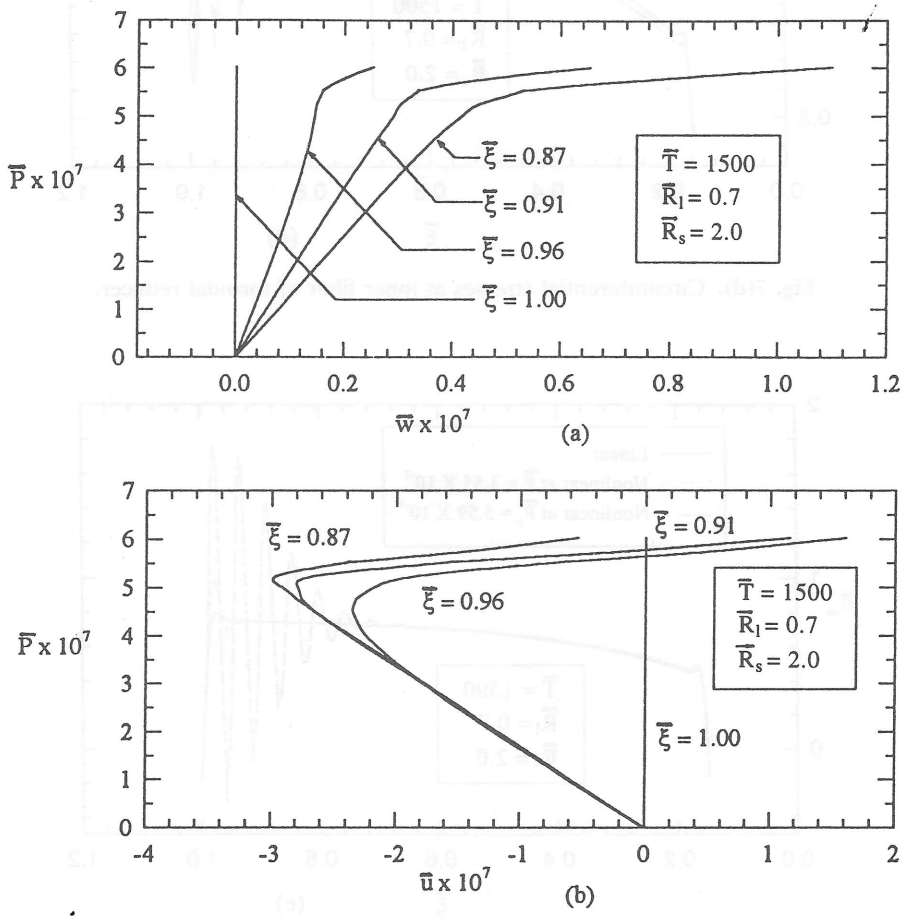

Fig. 7. (a) Axial displacements and (b) radial displacements.

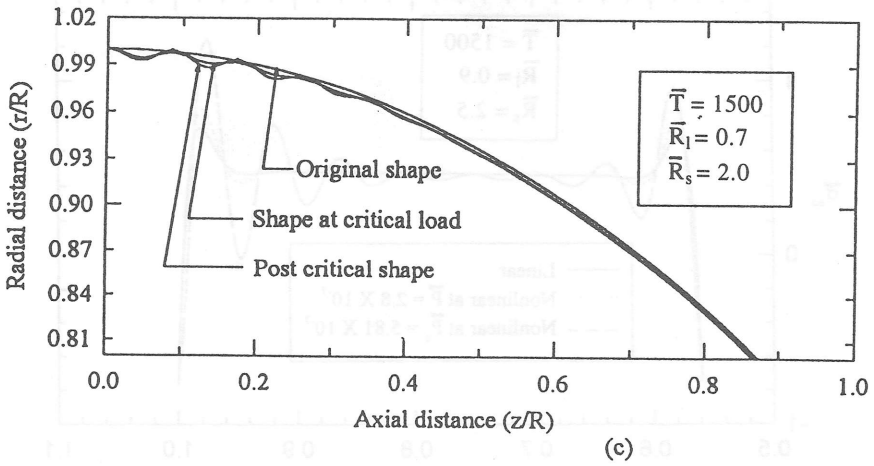

Fig. 7. (c). buckled configuration of toroidal reducer.

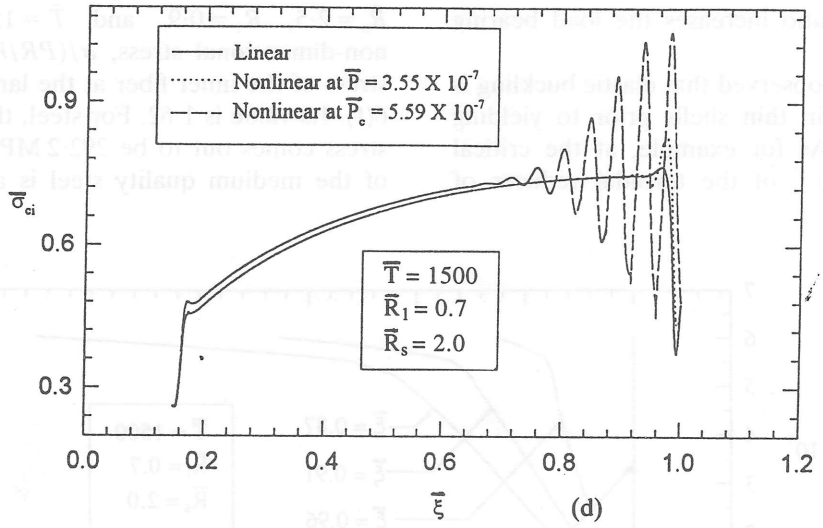

Fig. 7(d). Circumferential stresses at inner fiber of toroidal reducer.

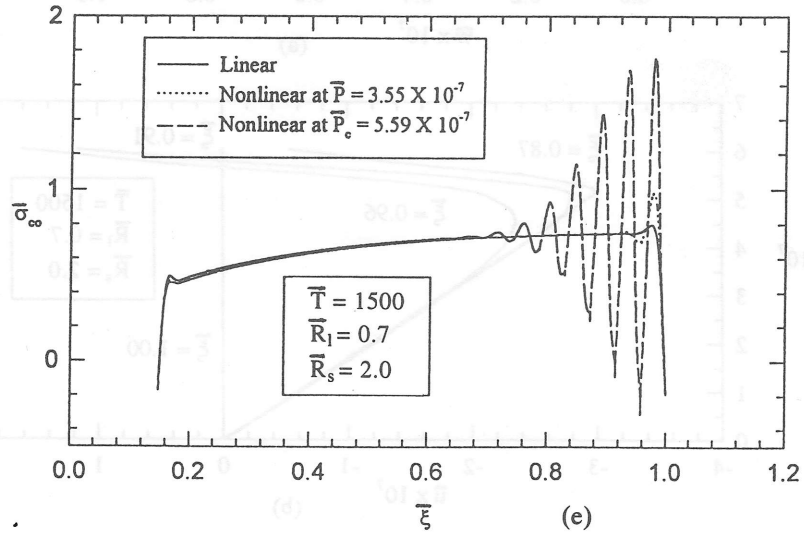

Fig. 7(e). Circumferential stresses at outer fiber of toroidal reducer.

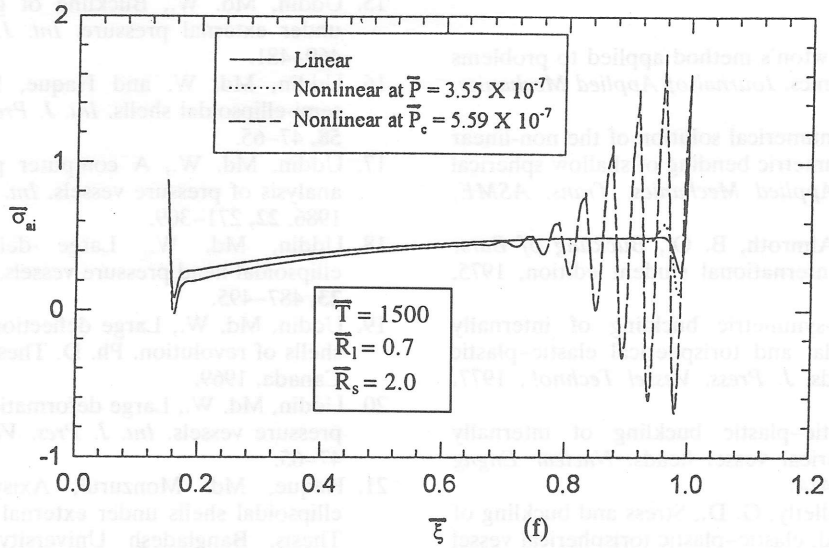

Fig. 7(f). Meridional stresses at inner fiber of toroidal reducer.

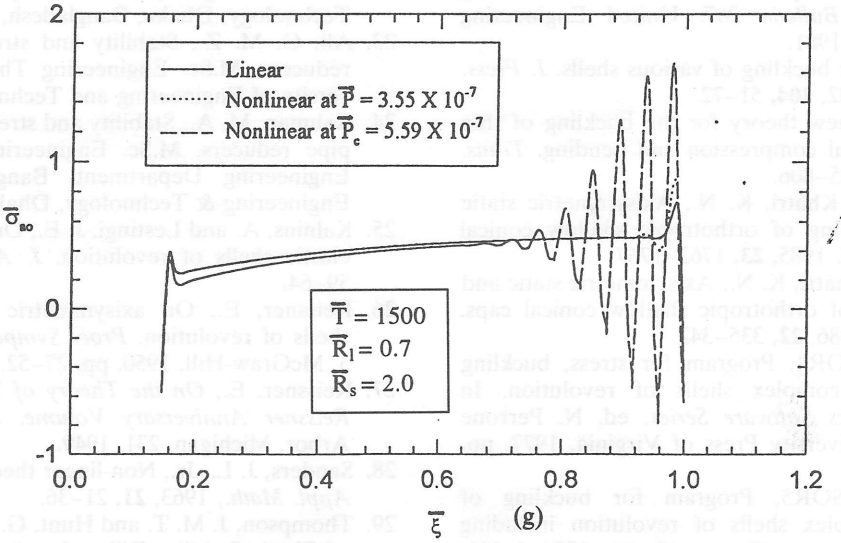

Fig. 7(g). Meridional stresses at outer fiber of toroidal reducer.

Therefore the induced maximum stress is well below the yield strength at this critical pressure.

CONCLUSION

From this investigation it may be concluded that toroidal pipe-reducers are far superior to conical reducers as they develop uniform stresses of lower magnitude under the same level of external loading. Regarding stability, toroidal reducers are superior to parabolic reducers at higher reduction ratio, but at lower reduction ratio, parabolic reducers can sustain higher load than toroidal reducers. It is also observed that toroidal reducers are much more stable than the conical reducers under uniform external pressure. The ratio of the critical pressure of a toroidal reducer to that of a conical reducer (with identical parameters) increases with increasing thickness ratio, increasing diameter ratio, and increasing curvature ratio. As curvature ratio increases, a toroidal reducer can sustain increasingly higher load than parabolic reducers of identical parameters. Keeping everything the same, a toroidal reducer of larger curvature ratio will be stronger than one with smaller curvature ratio.

It has been found that the regions near the fixed edges are most critically stressed. It has also been observed that long toroidal reducers (lower diameter ratios) are critically stressed near the larger end but this critical zone may also occur at the smaller end as the diameter ratio is gradually increased.

REFERENCES

1. Thurston, G. A., Newton's method applied to problems in non-linear mechanics. *Journal of Applied Mechanics,* 1965, 38–388.
2. Thurston, G. A., A numerical solution of the non-linear equations for axisymmetric bending of shallow spherical shells. *Journal of Applied Mechanics, Trans. ASME,* 1965, **28,** 557–562.
3. Brush, D. O. and Almroth, B. O., *Buckling of Bars, Plates and Shells,* International student edition, 1975, pp. 190–225.
4. Bushnell, D., Non-symmetric buckling of internally pressurized ellipsoidal and torispherical elastic–plastic pressure vessel heads. *J. Press. Vessel Technol.,* 1977, **99,** 54–63.
5. Bushnell, D., Elastic–plastic buckling of internally pressurized torispherical vessel heads. *Nuclear Engng Des.,* 1978, **48,** 405–414.
6. Bushnell, D. and Galletly, G. D., Stress and buckling of internally pressurized, elastic–plastic torispherical vessel heads—Comparison of tests and theory. *J. Press. Vessel Technol.,* 1977, **99,** 39–53.
7. Bushnell, D., Elastic–plastic buckling of internally pressurized ellipsoidal pressure vessel heads. *Welding Research Council Bulletin 267.* United Engineering Centre, New York, 1981.
8. Bushnell, D., Plastic buckling of various shells. *J. Press. Vessel Technol.,* 1982, **104,** 51–72.
9. Donnel, L. H., A new theory for the buckling of thin cylinders under axial compression and bending. *Trans. ASME,* 1934, **56,** 795–806.
10. Dumier, P. C. and Khatri, K. N., Axisymmetric static and dynamic buckling of orthotropic shallow conical caps. *AIAA Journal,* 1985, **23,** 1762–1767.
11. Dumir, P. C. and Khatri, K. N., Axisymmetric static and dynamic buckling of orthotropic shallow conical caps. *Comp. & Struct.,* 1986, **22,** 335–342.
12. Bushnell, D., BOSOR4, Program for stress, buckling and vibration of complex shells of revolution. In *Structural Mechanics Software Series,* ed. N. Perrone and W. Pilkey. University Press of Virginia, 1977, pp. 11–143.
13. Bushnell, D., BOSOR5, Program for buckling of elastic–plastic complex shells of revolution including large deflection and creep. *Comput. Struct.,* 1976, **6,** 221.
14. Almroth, B. O., Brogan, F. A. and Stanley, G. M., Structural analysis of general shells, Vol. 11. *User Instruction for STAGSC.* Lockhead Missiles & Space Co., Report LMSC-D633873, 1979.
15. Uddin, Md. W., Buckling of general spherical shells under external pressure. *Int. J. Mech. Sci.,* 1987, **29,** 469–481.
16. Uddin, Md. W. and Haque, Md. M., Instability of semi-ellipsoidal shells. *Int. J. Pres. Ves. & Piping,* 1994, **58,** 47–65.
17. Uddin, Md. W., A computer program for non-linear analysis of pressure vessels. *Int. J. Pres. Ves. & Piping,* 1986, **22,** 271–309.
18. Uddin, Md. W., Large deformation analysis of ellipsoidal head pressure vessels. *Comp. & Struct.,* 1986, **23,** 487–495.
19. Uddin, Md. W., Large deflection analysis of composite shells of revolution. Ph. D. Thesis, Carleton University, Canada, 1969.
20. Uddin, Md. W., Large deformation analysis of plate-end pressure vessels. *Int. J. Pres. Ves. & Piping,* 1987, **29,** 47–65.
21. Haque, Md. Monzurul, Axisymmetric buckling of ellipsoidal shells under external pressure. M.Sc. Engng Thesis, Bangladesh University of Engineering and Technology, Dhaka, Bangladesh, 1986.
22. Rahman, N. M. A., Axisymmetric buckling of imperfect ellipsoidal shells under external pressure. M.Sc. Engng Thesis, Bangladesh University of Engineering and Technology, Dhaka, Bangladesh, 1986.
23. Ali, G. M. Z., Stability and stress analysis of conical reducers. M.Sc. Engineering Thesis, Bangladesh University of Engineering and Technology, 1991.
24. Rahman, M. A., Stability and stress analysis of parabolic pipe reducers. M.Sc. Engineering Thesis, Mechanical Engineering Department, Bangladesh University of Engineering & Technology, Dhaka, Bangladesh, 1994.
25. Kalnins, A. and Lestingi, J. E., On non-linear analysis of elastic shells of revolution. *J. Appl. Mech.,* 1967, **34,** 59–64.
26. Reissner, E., On axisymmetric deformations of thin shells of revolution. *Proc. Symposia Appl. Math.,* Vol. 3. McGraw-Hill, 1950, pp. 27–52.
27. Reissner, E., *On the Theory of Thin Elastic Shells, H. Reissner Anniversary Volume.* J. W. Edwards, Ann Arbor, Michigan, 231, 1949.
28. Sanders, J. L., Jr., Non-linear theories for thin shells. *Q. Appl. Math.,* 1963, **21,** 21–36.
29. Thompson, J. M. T. and Hunt, G. W., *A General Theory of Elastic Stability.* Wiley, London, 1973.
30. Rahman, M. A. and Uddin, M. W., Stability analysis of parabolic pipe-reducer under uniform external pressure. *Int. J. Pres. Ves. & Piping,* 1993, **64,** 1–10.